Published in final edited form as:
Cell Stem Cell. 2013 February 7; 12(2): 215–223. doi:10.1016/j.stem.2012.11.021.

Secreted frizzled-related protein 3 regulates activity-dependent adult hippocampal neurogenesis

Mi-Hyeon Jang[1,2,3,*,#], **Michael A. Bonaguidi**[1,2,*], **Yasuji Kitabatake**[1,2,4,*], **Jiaqi Sun**[1,5,*], **Juan Song**[1,2], **Eunchai Kang**[1,2], **Heechul Jun**[1,3], **Chun Zhong**[1,2], **Yijing Su**[1,2], **Junjie U. Guo**[1,6], **Marie Xun Wang**[1], **Kurt A. Sailor**[1,6], **Ju-Young Kim**[1,2], **Yuan Gao**[1,7], **Kimberly M. Christian**[1,2], **Guo-li Ming**[1,2,6], and **Hongjun Song**[1,2,6,#]

[1]Institute for Cell Engineering, Johns Hopkins University School of Medicine, Baltimore, Maryland 21205, USA.

[2]Department of Neurology, Johns Hopkins University School of Medicine, Baltimore, Maryland 21205, USA.

[3]Department of Neurologic Surgery, Department of Biochemistry and Molecular Biology, Mayo College of Medicine, Rochester, Minnesota 55905, USA.

[4]Department of Pediatrics, Osaka University School of Medicine, 2-2 Yamadaoka, Suita, Osaka, 565-0871, Japan.

[5]School of Life Sciences, Tsinghua University, Beijing 100081, P.R. China.

[6]The Solomon H. Snyder Department of Neuroscience, Johns Hopkins University School of Medicine, Baltimore, Maryland 21205, USA.

[7]Lieber Institute for Brain Development, Johns Hopkins University School of Medicine, Baltimore, Maryland 21205, USA.

SUMMARY

Adult neurogenesis, a process of generating mature neurons from adult neural stem cells, proceeds concurrently with ongoing neuronal circuit activity and is modulated by various physiological and pathological stimuli. The niche mechanism underlying activity-dependent regulation of sequential steps of adult neurogenesis remains largely unknown. Here we report that neuronal activity decreases the expression of secreted frizzled-related protein 3 (sFRP3), a naturally secreted Wnt inhibitor highly expressed by adult dentate gyrus granule neurons. *Sfrp3* deletion activates quiescent radial neural stem cells and promotes newborn neuron maturation, dendritic growth and spine formation in the adult mouse hippocampus. Furthermore, *sfrp3* reduction is essential for activity-induced adult neural progenitor proliferation and acceleration of new neuron development. Our study identifies sFRP3 as an inhibitory niche factor from local mature dentate granule neurons that regulates multiple phases of adult hippocampal neurogenesis and suggests a

[#]Correspondence should be addressed to: Hongjun Song, Ph.D., Institute for Cell Engineering, Johns Hopkins University School of Medicine, 733 N. Broadway, MRB 759, Baltimore, MD 21205, USA. Tel: 443-287-7499, shongju1@jhmi.edu Mi-Hyeon Jang, Ph.D. jang.mihyeon@mayo.edu.
[*]These authors contributed equally to this work.

SUPPLEMENTAL INFORMATION

Supplementary information includes four figures, one table, supplemental experimental procedures and references.

novel activity-dependent mechanism governing adult neurogenesis via acute release of tonic inhibition.

INTRODUCTION

In the adult mammalian brain, active neurogenesis arises from neural stem cells in the subgranular zone (SGZ) of the dentate gyrus (Ming and Song, 2011). Radial glia-like precursors (RGLs) within the SGZ serve as one type of quiescent neural stem cell and continuously give rise to both dentate granule neurons and astrocytes in the adult mouse dentate gyrus (Bonaguidi et al., 2012). It is generally believed that the local neurogenic niche both houses neural stem cells and regulates their development; a number of niche components have been proposed, including blood vessels, astrocytes, ependymal cells and mature neurons (Ming and Song, 2011). For example, hippocampal astrocytes have been shown to instruct neuronal fate of cultured adult neural progenitors via Wnt signalling (Lie et al., 2005; Song et al., 2002). Lentivirus-mediated blockade of Wnt-signalling reduces immature new neuron number in the adult dentate gyrus and impairs hippocampus-dependent spatial and object recognition memory (Jessberger et al., 2009). Dysfunctional Wnt signalling also has been implicated in the age-related decline of hippocampal neurogenesis (Miranda et al., 2012). Endogenous Wnt ligands and inhibitors that are responsible for niche regulation of adult neurogenesis remain unclear.

Different from other somatic stem cell compartments, adult hippocampal neurogenesis proceeds concurrently with ongoing activity of existing neuronal circuits and is regulated by many physiological and pathological stimuli that affect neuronal activity, such as enriched environment, physical exercise, specific learning tasks and seizures (Ming and Song, 2011). For instance, seizures promote proliferation of adult dentate neural progenitors (Madsen et al., 2000; Parent et al., 1997) and accelerate maturation and integration of newborn neurons (Overstreet-Wadiche et al., 2006). These studies suggest the presence of stimulators and/or inhibitors that balance the magnitude and rate of adult neurogenesis in response to changes in existing neuronal circuit activity. Molecular identities of extrinsic factors, their niche sources and cellular targets that link circuit activity to adult neurogenesis are largely unknown.

In a search for activity-dependent extrinsic regulators of adult neurogenesis, we performed RNA-sequencing (RNA-seq) analysis of adult mouse dentate gyri with or without electroconvulsive stimulation (ECS), a paradigm that stimulates dentate circuits and promote progenitor proliferation and new neuron development during adult hippocampal neurogenesis (Ma et al., 2009; Madsen et al., 2000; Zhao et al., 2011). We found that the level of *secreted frizzled-related protein 3 (sfrp3)*, a gene highly expressed in the adult dentate gyrus, was significantly reduced by ECS (Figure 1A). Members of the sFRP family (sFRP1-5) can bind extracellular Wnt and thereby inhibit Wnt signalling (Jones and Jomary, 2002). Wnt signalling regulates diverse developmental processes in the embryonic brain and controls the proliferation and differentiation of progenitors in various adult tissues, including gut, hair follicle, bone, hematopoietic and nervous systems (Clevers and Nusse, 2012). Many Wnts retain their expression in the adult dentate gyrus (Shimogori et al., 2004). In this study, we identify sFRP3 as a novel inhibitory niche factor arising from mature dentate granule neurons to regulate neural stem cell quiescence and control the tempo of new neuron maturation in the adult hippocampus in an activity-dependent fashion.

RESULTS

sFRP3 limits dentate neural progenitor proliferation and new neuron production

To identify activity-dependent extrinsic regulators of adult neurogenesis, we examined expression profiles of all known Wnt inhibitors in the micro-dissected adult dentate gyrus tissue, including the sFRP family (sFRP1-5; Figure 1A), Dickkopf family (Dkk1-4), Wnt inhibitor factor (Wif1) and Cerberus (Cer1; Figure S1A). Notably, RNA-seq showed high levels of *sfrp3 and Dkk3* expression, but only *sfrp3* expression was significantly altered by ECS. In situ analysis revealed specific and high levels of *sfrp3* expression in the dentate granule cell layer, but not the SGZ of adult mice (Figure 1B), whereas high levels of *dkk3* expression were limited to nearby CA3 neurons (Thompson et al., 2008). In adult *nestin-GFP* mice, minimal *sfrp3* expression was detected in GFP^+ neural progenitors and their immature progeny in the adult dentate gyrus (Figure 1C), a result consistent with recent expression profiling of purified neural progenitors and immature neurons from adult mouse dentate gyrus (Bracko et al., 2012).

To assess the potential role of sFRP3 in adult hippocampal neurogenesis, we obtained *sfrp3* knockout (KO) mice (Figure S1B). Adult *sfrp3* heterozygous (HET) and homozygous KO mice were grossly normal without any detectable developmental defects (data not shown). Adult mice were injected once with BrdU (200 mg/kg body weight, i.p.) to label cells during the Sphase of the cell cycle and sacrificed 2 hours later. Stereological quantification showed a significant increase in the $BrdU^+$ cell density in the SGZ of adult *sfrp3* KO mice compared to wild-type (WT) or HET littermates (Figure 1D). Analysis using endogenous cell proliferation marker MCM2 showed similar results (Figure 1E). To rule out potential developmental contributions from *sfrp3* germ-line deletion, we developed lentiviruses and AAVs to acutely knock down endogenous sFRP3 expression adult WT mice (Figure S1C). Fourteen days after stereotaxic injection of lentiviruses co-expressing shRNA-*sfrp3* and tdTomato into the dentate gyrus, stereological quantification showed a significant increase of $BrdU^+$ cells in the SGZ compared to shRNA-control (Figure S1D). Consistent with the notion that sFRP3 inhibits Wnt signalling (Jones and Jomary, 2002), TOPGAL reporter mice, which drives a LacZ gene under the control of a LEF/TCF and b-catenin inducible promoter to report canonical Wnt signalling (Figure S1E) (DasGupta and Fuchs, 1999), showed a significant increase in the number of βGalactosidase-expressing (βGal^+) cells within the adult dentate gyrus upon *sfrp3* knockdown (Figure S1E). Together, these results suggest that sFRP3 functions to suppress neural progenitor proliferation via inhibition of Wnt signalling.

To determine whether differences in neural progenitor proliferation lead to a net change in the number of mature adult-born neurons, we injected adult mice with BrdU (50 mg/kg body weight, i.p.) once daily for 7 days and examined the expression of mature neuronal marker NeuN in $BrdU^+$ cells 28 days after the first BrdU injection (Figure 1F). The density of $BrdU^+NeuN^+$ mature newborn neurons in the dentate gyrus of adult KO mice was significantly higher than that in WT littermates. Thus, sFRP3 limits neuronal production during adult hippocampal neurogenesis.

sFRP3 regulates quiescence, but not lineage choice, of dentate radial glia-like neural stem cells

The BrdU and MCM2 results indicate an increase of IPCs in adult *sfrp3* KO mice, which constitute the large majority of dividing cells in the adult SGZ. This increase may result from changes in IPC proliferation or IPC production from RGLs. To determine the cellular target of sFRP3, we assessed RGL proliferation by identifying co-localization of MCM2 and SGZ $nestin^+$ cells with radial processes within the adult SGZ (Figure S2A). Stereological

quantification showed that *sfrp3* KO mice exhibited a 45% increase of activated RGLs at the population level (Figure S2B).

To directly determine whether *sfrp3* deletion affects quiescent neural stem cell activation and their lineage choice in the adult SGZ, we performed short-term in vivo clonal analysis (Bonaguidi et al., 2011). We generated *nestin-CreER^{T2}::Z/EG$^{f/+}$::sfrp3$^{-/-}$* (KO) and *nestin-CreER^{T2}::Z/EG$^{f/+}$::sfrp3$^{+/+}$* mice (control; Figure S2C). We injected a single low dose of tamoxifen (62 mg/kg body weight, i.p.) into adult mice for induction, an approach we previously showed to sparsely label mostly MCM2^{-} quiescent RGLs in the adult SGZ (Figure S2D) (Bonaguidi et al., 2011). At 7 days post injection (dpi), we quantified RGL quiescence or activation status according to the absence (quiescent) or presence (active) of progeny adjacent to the RGL within individual GFP^{+} clones (Figures 2A-D). Adult KO mice exhibited a significant decrease in the percentage of clones with a single RGL (Figure 2E), suggesting that sFRP3 suppresses the activation of quiescent RGLs in the adult SGZ. By 7 dpi, activated RGLs could be observed generating IPCs, astroglia or additional RGLs (Figures 2B-D). Interestingly, percentages of each type of activated clones were similar between WT and KO mice (Figure 2F), suggesting that *sfrp3* deletion does not alter RGL lineage choice upon activation. These results support a model that sFRP3 suppresses RGL activation in the adult dentate gyrus.

sFRP3 suppresses the tempo of newborn neuron maturation in the adult hippocampus

Wnt-signalling is known to be active in immature neurons in the adult hippocampus (Lie et al., 2005; Madsen et al., 2003), therefore we examined whether sFRP3 also regulates newborn neuron development. The maturation status of newborn neurons can be defined by the sequential and partially overlapping expression of immature neuron marker DCX and mature neuron marker NeuN (Figure S3A). Adult mice were injected with BrdU (50 mg/kg body weight, i.p.) once daily for 1 week and analyzed 2 weeks after the first BrdU injection. Quantitative analysis showed a significant decrease in the percentage of DCX^{+}NeuN^{-} immature neurons with a concurrent increase in the percentage of more developed DCX^{+}NeuN^{+} neurons among all BrdU^{+} cells in KO mice compared to WT littermates (Figures 3A-B). Thus, *sfrp3* deletion leads to accelerated maturation of newborn neurons in the adult dentate gyrus.

To further characterize the role of sFRP3 in neuronal development, we examined dendritic outgrowth of newborn neurons in adult mice using a GFP-expressing retrovirus for birth-dating and genetic labeling of proliferating progenitors and their progeny (Ge et al., 2006). Quantitative analysis showed significant increases in both total dendritic length and branch number of GFP^{+} newborn neurons in adult KO mice compared to their WT littermates at 14 dpi (Figures 3C-D). Interestingly, GFP^{+} newborn neurons in the HET and KO mice exhibited similarly accelerated dendritic growth compared to WT littermates (Figures 3C-D), suggesting that dendritic development of newborn neurons is particularly sensitive to sFRP3 levels. At 21 dpi, GFP^{+} neurons in KO mice still exhibited significantly increased total dendritic length and branch number compared to those in WT littermates, although the differences were smaller compared to those at 14 dpi (Figures 3E-F). Interestingly, GFP^{+} neurons in KO mice also displayed significantly increased dendritic spine density compared to those in WT littermates at 21 dpi (Figures 3G-H). Thus, *sfrp3* deletion leads to increased tempo of multiple processes of neuronal maturation during adult hippocampal neurogenesis, from dendritic outgrowth to spine formation of newborn neurons.

To examine whether an acute decrease of sFRP3 levels also regulate newborn neurons, we stereotaxically injected lentiviruses co-expressing tdTomato and shRNA-*sfrp3* or shRNA-control, followed by injection of retroviruses expressing GFP into the dentate gyrus of adult WT mice (Figure S3B). Analysis of GFP^{+} newborn neurons at 14 dpi showed increased total

dendritic length and branch numbers upon shRNA-*sfrp3* expression compared to shRNA-control (Figures S3B-D). Few GFP^+ neurons were $tdTomato^+$, further supporting a non cell autonomous effect of sFRP3. Together, these results suggest an inhibitory role of sFRP3 in regulating newborn neuron maturation in the adult dentate gyrus.

sFRP3 regulates neuronal activity-induced adult hippocampal neurogenesis

The activity-dependent expression profile of sFRP3 and its role in adult neurogenesis prompted us to assess whether it serves as a substrate for activity-dependent modulation of adult neurogenesis. We examined the magnitude and time course of *sfrp3* expression in response to dentate gyrus activation using in situ hybridization and quantitative real-time PCR analyses. The level of dentate *sfrp3* expression was reduced to about 50% of those in sham controls 1 day after ECS and gradually returned to basal levels within 7 days (Figure 4A). Exercise, a physiological stimulation that activates dentate granule neurons as indicated by Arc expression, also led to significantly decreased *sfrp3* expression (Figure 4B) and increased Wnt signalling (Figure S4A). To examine whether direct neuronal activation is sufficient to affect *sfrp3* expression, we stereotaxically injected engineered AAV expressing ChR2-YFP into the adult dentate gyrus, followed by light stimulations three weeks later. Indeed, direct and strong activation of dentate granule neurons, as indicated by Arc expression, led to a significant decrease of *sfrp3* expression in the dentate granule neurons (Figure S4B). Furthermore, pathological stimulation with pilocarpine-induced seizures resulted in prolonged decrease of *sfrp3* expression (Figure S4C). These results indicate that *sfrp3* expression in the adult dentate gyrus is regulated by multiple forms of neuronal activity in vivo.

We next examined the impact of *sfrp3* deletion on sequential steps of adult neurogenesis in response to dentate gyrus activation. We subjected adult *sfrp3* KO mice and WT littermates to a single ECS and analyzed progenitor proliferation 3 days later with BrdU injection (Figure 4C). Interestingly, the ECS-induced increase of progenitor proliferation was attenuated from 87% in WT mice to 28% in *sfrp3* KO littermates (Figures 4C and S4D), suggesting significant occlusion of ECS-induced increase of progenitor proliferation by *sfrp3* deletion. Notably, the lack of further increase by ECS in adult *sfrp3* KO mice was not due to a ceiling effect on progenitor proliferation because WT mice exhibited even higher number of $BrdU^+$ cells after running (Figure 4E). Importantly, infusion of recombinant sFRP3 protein into the dentate gyrus of adult WT mice abolished the ECS-induced increase of neural progenitor proliferation (Figure 4D), suggesting that reduction of sFRP3 levels is required for the ECS-induced increase of progenitor proliferation. In addition to ECS, the voluntary running-induced increase of progenitor proliferation was attenuated from 188% in WT mice to 47% in KO littermates (Figures 4E and S4E). Together, these results suggest that sFRP3, at least in part, mediates activity-induced neural progenitor proliferation in the adult dentate gyrus.

To address whether *sfrp3* is also involved in ECS-induced acceleration of new neuron development during adult neurogenesis, we subjected WT mice to a single ECS either 3 or 6 days after retroviral injection. Morphological assessment at 14 dpi demonstrated that ECS at both time points increased total dendrite length and branch number of GFP^+ newborn neurons (Figures S4F-G). In contrast, ECS had no effect on dendritic growth of GFP^+ newborn neurons in adult *sfrp3* KO (Figures 4F and S4H). Thus, *sfrp3* deletion also occludes neuronal activity-induced acceleration of new neuron dendritic development in the adult dentate gyrus.

DISCUSSION

A fundamental question in stem cell biology is whether and how niche signals couple changing tissue demands with somatic stem cell activity to promote functional homeostasis. Unique among adult somatic tissues, neural stem cells reside within an active neuronal network, where the local neuronal activity could serve as an effective readout of current tissue demands and provide signals to tune the magnitude and tempo of neurogenesis. Our study identifies sFRP3 as a neuronal activity-regulated niche factor from mature dentate granule neurons that exhibits control over multiple steps of adult hippocampal neurogenesis, from activation of quiescent adult neural stem cells, to maturation, dendritic development and spine formation of newborn dentate granule neurons. Our results suggest a new mode of dynamic regulation of adult neurogenesis via acute release of tonic inhibition.

Little is known about niche mechanisms regulating quiescent neural stem cells, largely because of a lack of effective approaches to examine this population of precursors. Using a genetic sparse labelling approach for clonal analysis of stem cell division and lineage choice (Bonaguidi et al., 2011), we show that sFRP3 deletion increases quiescent neural stem cell activation in the adult hippocampus and, surprisingly, has no effect on the frequency of symmetric and asymmetric neurogenic or gliogenic cell division. Thus, in contrast to a prominent role of Wnt signalling in promoting neuronal fate commitment of proliferating multipotent adult neural progenitors in vitro (Lie et al., 2005), sFRP3 does not affect the lineage choice of quiescent nestin^{+} radial glia-like neural stem cells within the adult hippocampus in vivo. Interestingly, sFRP3 inhibits both quiescent neural stem cell activation and maturation of their neuronal progeny. This activity-driven, coordinated regulation of sequential processes suggests that sFRP3 may be both a sensor and effector for the homeostatic regulation of adult neurogenesis.

While Wnt-signalling has been shown to control proliferation and differentiation of progenitors in many adult tissues (Clevers and Nusse, 2012), little is known about functions of various naturally secreted Wnt inhibitors in adult stem cell biology in vivo. Consistent with a role as a broad Wnt signalling inhibitor in the adult brain, sFRP3 reduction leads to increased canonical Wnt signalling in the adult dentate gyrus as indicated by TOPGAL reporter activation. Interestingly, endogenous *sfrp3* expression in the dentate gyrus is reduced by therapeutic (ECS), physiological (voluntary running), pathological stimuli (seizures) and direct neuronal activation, suggesting that sFPR3 is a key sensor of various external stimuli within dentate granule neurons in vivo. The presence of potent negative regulators, such as sFRP3, may also be of significant physiological importance to keep the process of adult neurogenesis in balance. For example, pathological activation of neuronal circuitry by chronic seizures, which leads to a sustained decrease in *sfrp3* expression, causes aberrant outgrowth of newborn neurons and formation of recurrent connections that may contribute to epileptogenesis (Jessberger et al., 2007; Parent et al., 1997). Recent studies have also suggested significant depletion of neural stem cells upon their activation in the adult dentate gyrus (Bonaguidi et al., 2012). For example, deletion of BMPR1A/SMAD4, PTEN, RBPJk, or REST/NRSF in adult neural stem cells all lead to initial activation and subsequent depletion of the stem cell pool and reduced levels of continuous adult hippocampal neurogenesis. Therefore, a tightly controlled dynamic range of Wnt signalling via inhibitor levels may fine-tune adult neural stem cell behaviour to meet changing local tissue demands, while globally maintaining the stem cell pool over long-term, a mechanism that may be generalizable to regulation of other stem cells.

In summary, our study suggests a model in which physiological experience and pathological stimuli, via neuronal activity, modulate *sfrp3* expression in dentate granule neurons to regulate quiescent neural stem cell activation and development of their progeny by fine-

tuning Wnt signalling. Given the critical contribution of adult neurogenesis to brain plasticity, learning and memory, and brain disorders, identification of sFRP3 as an activity-dependent inhibitory niche factor have significant and broad implications.

EXPERIMENTAL PROCEDURES

RNA-seq, Quantitative Real-Time PCR, and *in situ* Hybridization

Total poly-A-containing mRNA was immediately isolated after dissection of dentate gyrus from hippocampi to create the cDNA library for Illumina HiSeq2000 sequencing. Pair-end reads (97 bp) of cDNA sequences were aligned to mouse reference genome mm9 by TopHat47 with reference gene annotations. Relative abundances of each transcript were estimated by Cufflinks48 using Ensemble gene annotation (Build NCBIM37).

Quantitative real-time PCR was performed in triplicate using following primers were used: GAPDH: 5′- GTATTGGGCGCCTGGTCACC-3′ (forward), 5′- CGCTCCTGGAAGATGGTGATGG-3′ (reverse); sFRP3: 5′- CAAGGGACACCGTCAATCTT-3′ (forward), 5′- CATATCCCAGCGCTTGACTT-3′ (reverse).

In situ hybridization analysis was performed using the digoxygenin-labeled antisense RNA corresponding to the full-length coding sequence of *sfrp3* as previously described (Ma et al., 2009). All experiments were processed in parallel for direct comparison of labelling.

Electroconvulsive Stimulation, Voluntary Running, Pilocarpine Treatment and Optogenetic Manipulation

Animals were administered ECS as previously described (Ma et al., 2009). Sham control animals received the same treatment, except that no current was passed. For voluntary running experiments, animals were randomly separated into two groups in standard home cages with free access to a functional or locked running wheel mounted in the cage as described previously (Guo et al., 2011; Ma et al., 2009). For pilocarpine-induced seizure, adult female WT mice were i.p. administered of methylscopolamine (2 mg/kg body weight), followed by pilocarpine (320 mg/kg body weight) 30 minutes later. Control mice were administered a comparable volume of vehicle after the initial methylscopolamine treatment. Only mice that had multiple level III–V seizures within 2 hours of pilocarpine injection were used (Shibley and Smith, 2002). For optogenetic manipulation, fiber optic cannulae (Doric Lenses, Inc.) were implanted at same sites right after AAV injection with the dorsal-ventral depth of 1.6 mm from the skull and let recover for three weeks as previously described (Song et al., 2012). A light stimulation protocol (472 nm; 15 ms at 20 Hz for 3 min) (Liu et al., 2012) was applied via the DPSSL laser system (Laser Century Co. Ltd.) twice 4 days apart similarly as previously described (Song et al., 2012). Animals were processed for dual *sfrp3* in situ and Arc immunostaining 2 hours after the second light stimulation. All animal procedures were approved by the Institutional Animal Care and Use Committee.

BrdU Labelling, Immunostaining, Confocal Imaging and Analysis

Adult littermates of adult female *sfrp3* WT and KO (7–8 weeks old) were i.p. injected once with BrdU (200 mg/kg body weight) and analyzed 2 hours later. For neuronal differentiation and maturation analysis, adult littermates were injected with BrdU (50 mg/kg body weight, once daily at 10 AM) for one week and sacrificed two or four weeks after the first BrdU injection. Coronal brain sections (40 μm thick) were prepared from injected mice and processed for immunostaining and confocal imaging as previously described (Bonaguidi et al., 2011; Ge et al., 2006). Antibodies used in this study are listed in Table S1. Stereological quantification within the SGZ and granule cell layer were carried out as previously

described (Kempermann et al., 1997). All assessments were performed by an observer blind to genotypes or treatments. Statistic significance ($P < 0.01$) was assessed using one-way ANOVA or student's t-test as indicated.

Production and Stereotaxic Injection of Engineered Viruses and Osmotic Pump Infusion

Engineered self-inactivating murine onco-retroviruses were used to express GFP specifically in proliferating cells and their progeny following stereological injection and processed at 14 or 21 dpi for morphological analysis as previously described (Ge et al., 2006). Summaries of total dendritic length, branch number and spine densities of each individual neuron under different conditions are shown in cumulative distribution plots. Statistical significance ($P < 0.01$) was assessed using the Kolmogorov-Smirnov test.

A lentiviral vector pFUGW co-expressing shRNA under the U6 promoter and tdTomato under the EF1α promoter were stereotaxically injected into the dentate gyrus of adult W mice. The short hairpin sequences used are as follows: (shRNA-*sfrp3*) 5'-GCTAGCGATTCCACTCAGAAT-3'; (shRNA-control) 5'-AGTTCCAGTACGGCTCCAA-3'. For cell proliferation analysis, BrdU (200 mg/kg body weight) was injected 14 days after lentiviral infection and examined 2 hours later. Stereological quantification of $BrdU^+$ cells in the SGZ were carried out only in $tdTomato^+$ coronal sections. For dendritic development analysis, retroviruses expressing GFP were injected into same sites 14 days after lentiviral injection and mice were examined 14 days later for morphological analysis. An AAV vector co-expressing the same shRNA under the U6 promoter and GFP under the EF1α promoter (Guo et al., 2011) was used in adult TOPGAL reporter mice to examine the role of sFRP3 in Wnt signalling.

For optogenetic manipulation, engineered AAV expressing ChR2-YFP under the EF1α promoter were obtained from Viral Core of University of Pennsylvania and stereotaxically injected into the dentate gyrus of adult WT mice using following coordinates (in mm): posterior = −2 from Bregma; lateral = ±1.5; ventral = 2.2.

For sFRP3 infusion experiments, adult WT animals were infused with recombinant sFRP3 (120 ng/day; R&D systems) into the right ventricle by osmotic minipumps (Alzet) for 7 days with following coordinates (in mm: posterior = 0.34 from Bregma, lateral = 1, ventral = 3) (Guo et al., 2011). Animals were subject to a single ECS at day 4, injected with BrdU (200 mg/kg body weight) at day 7, and then analyzed at 2 hours after BrdU injection.

Animals, Tamoxifen Administration, and Clonal Analysis

TOPGAL reporter mice (JAX 004623) (DasGupta and Fuchs, 1999) were used to monitor canonical Wnt signalling. Nestin-GFP mice (Song et al., 2012) were used for dual *sfrp3* in situ and GFP immunohistology analysis. For clonal analysis, *nestin-CreER*$^{T2+/-}$*::Z/EG*$^{f/+}$*::sfrp3*$^{-/-}$ mice and *nestin-CreER*$^{T2+/1}$*::Z/EG*$^{f/+}$*::sfrp3*$^{+/+}$ controls were used. A single low dose of tamoxifen injection (62 mg/kg body weight, i.p.; Sigma) into 2 month-old mice resulted in sparse labeling at the clonal level for analysis at 7 dpi in both control and *sfrp3* KO mice as previously described (Bonaguidi et al., 2011).

Supplementary Material

Refer to Web version on PubMed Central for supplementary material.

Acknowledgments

We thank Drs. D. Ginty, S. Jessberger, X. He, and members of Song and Ming laboratories for suggestions, A. Rattner and J. Nathans for generating *sfrp3* KO mice, J.H. Shin and B. Xie for help with RNA-seq, and P. Worley

for Arc antibodies and initial help with ECS. This work was supported by NARSAD and NIH (NS047344, MH087874, ES021957) to H.S., NIH (NS048271, HD069184) and NARSAD to G-l.M., NIH (MH090115) and NARSAD to M-H.J., NIH (NS080913) to M.A.B., and by Postdoctoral Fellowship Awards from MSCRF to J.S., E.K., Y.S. and K.C.

REFERENCES

Bonaguidi MA, Song J, Ming GL, Song H. A unifying hypothesis on mammalian neural stem cell properties in the adult hippocampus. Curr Opin Neurobiol. 2012

Bonaguidi MA, Wheeler MA, Shapiro JS, Stadel RP, Sun GJ, Ming GL, Song H. In vivo clonal analysis reveals self-renewing and multipotent adult neural stem cell characteristics. Cell. 2011; 145:1142–1155. [PubMed: 21664664]

Bracko O, Singer T, Aigner S, Knobloch M, Winner B, Ray J, Clemenson GD Jr, Suh H, Couillard-Despres S, Aigner L, et al. Gene expression profiling of neural stem cells and their neuronal progeny reveals IGF2 as a regulator of adult hippocampal neurogenesis. J Neurosci. 2012; 32:3376–3387. [PubMed: 22399759]

Clevers H, Nusse R. Wnt/beta-catenin signaling and disease. Cell. 2012; 149:1192–1205. [PubMed: 22682243]

DasGupta R, Fuchs E. Multiple roles for activated LEF/TCF transcription complexes during hair follicle development and differentiation. Development. 1999; 126:4557–4568. [PubMed: 10498690]

Ge S, Goh EL, Sailor KA, Kitabatake Y, Ming GL, Song H. GABA regulates synaptic integration of newly generated neurons in the adult brain. Nature. 2006; 439:589–593. [PubMed: 16341203]

Guo JU, Ma DK, Mo H, Ball MP, Jang MH, Bonaguidi MA, Balazer JA, Eaves HL, Xie B, Ford E, et al. Neuronal activity modifies the DNA methylation landscape in the adult brain. Nat Neurosci. 2011; 14:1345–1351. [PubMed: 21874013]

Guo JU, Su Y, Zhong C, Ming GL, Song H. Hydroxylation of 5- methylcytosine by TET1 promotes active DNA demethylation in the adult brain. Cell. 2011; 145:423–434. [PubMed: 21496894]

Jessberger S, Clark RE, Broadbent NJ, Clemenson GD Jr, Consiglio A, Lie DC, Squire LR, Gage FH. Dentate gyrus-specific knockdown of adult neurogenesis impairs spatial and object recognition memory in adult rats. Learn Mem. 2009; 16:147–154. [PubMed: 19181621]

Jessberger S, Zhao C, Toni N, Clemenson GD Jr, Li Y, Gage FH. Seizure-associated, aberrant neurogenesis in adult rats characterized with retrovirus-mediated cell labeling. J Neurosci. 2007; 27:9400–9407. [PubMed: 17728453]

Jones SE, Jomary C. Secreted Frizzled-related proteins: searching for relationships and patterns. Bioessays. 2002; 24:811–820. [PubMed: 12210517]

Kempermann G, Kuhn HG, Gage FH. More hippocampal neurons in adult mice living in an enriched environment. Nature. 1997; 386:493–495. [PubMed: 9087407]

Lie DC, Colamarino SA, Song HJ, Desire L, Mira H, Consiglio A, Lein ES, Jessberger S, Lansford H, Dearie AR, Gage FH. Wnt signalling regulates adult hippocampal neurogenesis. Nature. 2005; 437:1370–1375. [PubMed: 16251967]

Liu X, Ramirez S, Pang PT, Puryear CB, Govindarajan A, Deisseroth K, Tonegawa S. Optogenetic stimulation of a hippocampal engram activates fear memory recall. Nature. 2012; 484:381–385. [PubMed: 22441246]

Ma DK, Jang MH, Guo JU, Kitabatake Y, Chang ML, Pow-Anpongkul N, Flavell RA, Lu B, Ming GL, Song H. Neuronal activity-induced Gadd45b promotes epigenetic DNA demethylation and adult neurogenesis. Science. 2009; 323:1074–1077. [PubMed: 19119186]

Madsen TM, Treschow A, Bengzon J, Bolwig TG, Lindvall O, Tingstrom A. Increased neurogenesis in a model of electroconvulsive therapy. Biol Psychiatry. 2000; 47:1043–1049. [PubMed: 10862803]

Ming GL, Song H. Adult neurogenesis in the mammalian brain: significant answers and significant questions. Neuron. 2011; 70:687–702. [PubMed: 21609825]

Miranda CJ, Braun L, Jiang Y, Hester ME, Zhang L, Riolo M, Wang H, Rao M, Altura RA, Kaspar BK. Aging brain microenvironment decreases hippocampal neurogenesis through Wnt-mediated survivin signaling. Aging Cell. 2012; 11:542–552. [PubMed: 22404871]

Overstreet-Wadiche LS, Bromberg DA, Bensen AL, Westbrook GL. Seizures accelerate functional integration of adult-generated granule cells. J Neurosci. 2006; 26:4095–4103. [PubMed: 16611826]

Parent JM, Yu TW, Leibowitz RT, Geschwind DH, Sloviter RS, Lowenstein DH. Dentate granule cell neurogenesis is increased by seizures and contributes to aberrant network reorganization in the adult rat hippocampus. J Neurosci. 1997; 17:3727–3738. [PubMed: 9133393]

Shibley H, Smith BN. Pilocarpine-induced status epilepticus results in mossy fiber sprouting and spontaneous seizures in C57BL/6 and CD-1 mice. Epilepsy Res. 2002; 49:109–120. [PubMed: 12049799]

Song H, Stevens CF, Gage FH. Astroglia induce neurogenesis from adult neural stem cells. Nature. 2002; 417:39–44. [PubMed: 11986659]

Song J, Zhong C, Bonaguidi MA, Sun GJ, Hsu D, Gu Y, Meletis K, Huang ZJ, Ge S, Enikolopov G, et al. Neuronal circuitry mechanism regulating adult quiescent neural stem-cell fate decision. Nature. 2012; 489:150–154. [PubMed: 22842902]

Thompson CL, Pathak SD, Jeromin A, Ng LL, MacPherson CR, Mortrud MT, Cusick A, Riley ZL, Sunkin SM, Bernard A, et al. Genomic anatomy of the hippocampus. Neuron. 2008; 60:1010–1021. [PubMed: 19109908]

Zhao C, Warner-Schmidt J, Duman RS, Gage FH. Electroconvulsive seizure promotes spine maturation in newborn dentate granule cells in adult rat. Dev Neurobiol. 2011; 72:937–942. [PubMed: 21976455]

Highlights

- Wnt inhibitor sFRP3 exhibits activity-dependent expression in the adult hippocampus
- sFRP3 maintains quiescence of adult hippocampal radial glia-like neural stem cells
- sFRP3 inhibits maturation, dendritic development and spine formation of new neurons
- sFRP3 partially mediates activity-dependent adult hippocampal neurogenesis

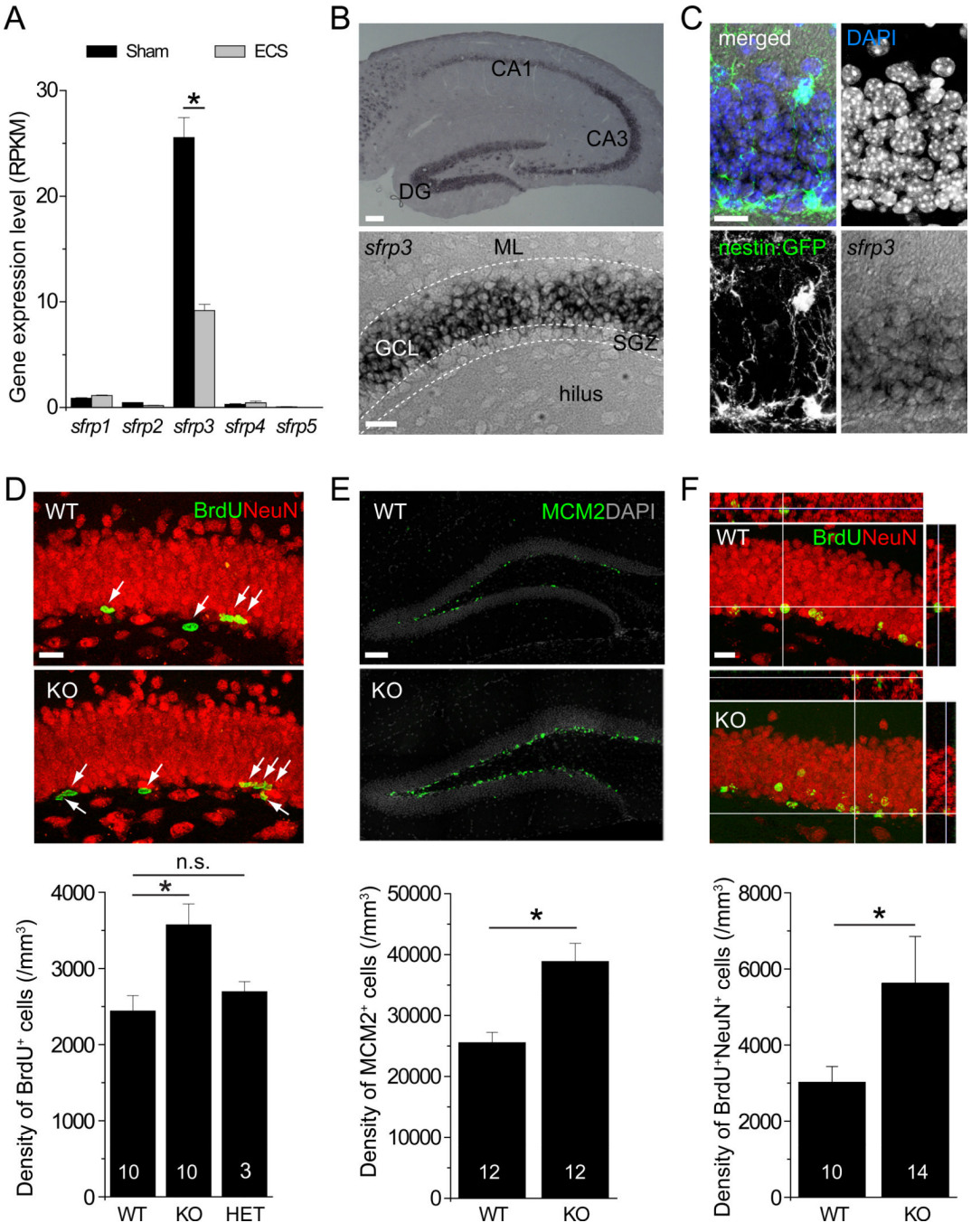

Figure 1. *sfrp3* Expression and Regulation of Neurogenesis in the Adult Hippocampus

(A) RNA-seq quantification of *sfrp1-5* expression in micro-dissected dentate gyri of adult wide-type (WT) mice 0 or 4 hours after a single ECS. Values represent mean ± SEM (n = 3; *: $P < 0.01$; one-way ANOVA). RPKM: reads per kilobase of exon per million fragments mapped.

(B-C) *sfrp3* expression in the adult mouse hippocampus. Shown in (B) are sample in situ images of *sfrp3* expression in the whole hippocampus (top; scale bar: 100 μm) and dentate gyrus (bottom; scale bar: 20 μm). Note *sfrp3* expression of in the granule cell layer (GCL), but not in the SGZ (bottom). ML: molecular layer. Shown in (C) are sample dual *sfrp3* in

situ and GFP immunostaining of the dentate gyrus of adult *nestin-GFP* mice. Scale bar: 20 μm.

(D-F) Increased progenitor proliferation and newborn neuron number in the dentate gyrus of adult *sfrp3* KO mice. In (D), animals were injected with BrdU and analyzed 2 hours later. Shown are sample projected confocal images of BrdU immunostaining (arrows) in the dentate gyrus of adult *sfrp3* KO and WT littermate (top; scale bar: 50 μm) and stereological quantification of $BrdU^+$ cells in the SGZ of adult WT, HET and KO littermates (bottom). Number associated with bar graphs indicates the number of animals examined. Values represent mean ± SEM (*: $P < 0.01$; n.s.: $P > 0.1$; one-way ANOVA). Shown in (E) are sample projected confocal images of MCM2 immunostaining and DAPI staining in the dentate gyrus (top; scale bar: 100 μm) and stereological quantification of $MCM2^+$ cells. Values represent mean ± SEM (*: $P < 0.05$; student's t-test). In (F), adult mice were injected with BrdU once daily for one week and examined four weeks after the first BrdU injection. Shown are sample projected confocal images of BrdU and NeuN immunostaining (top). Orthogonal views are shown to confirm co-localization of BrdU and NeuN. Scale bar: 50 μm. Also shown is stereological quantification of $NeuN^+BrdU^+$ mature newborn neurons (bottom). Values represent mean ± SEM (*: $P < 0.01$; student's t-test).

See also Figure S1 and Table S1.

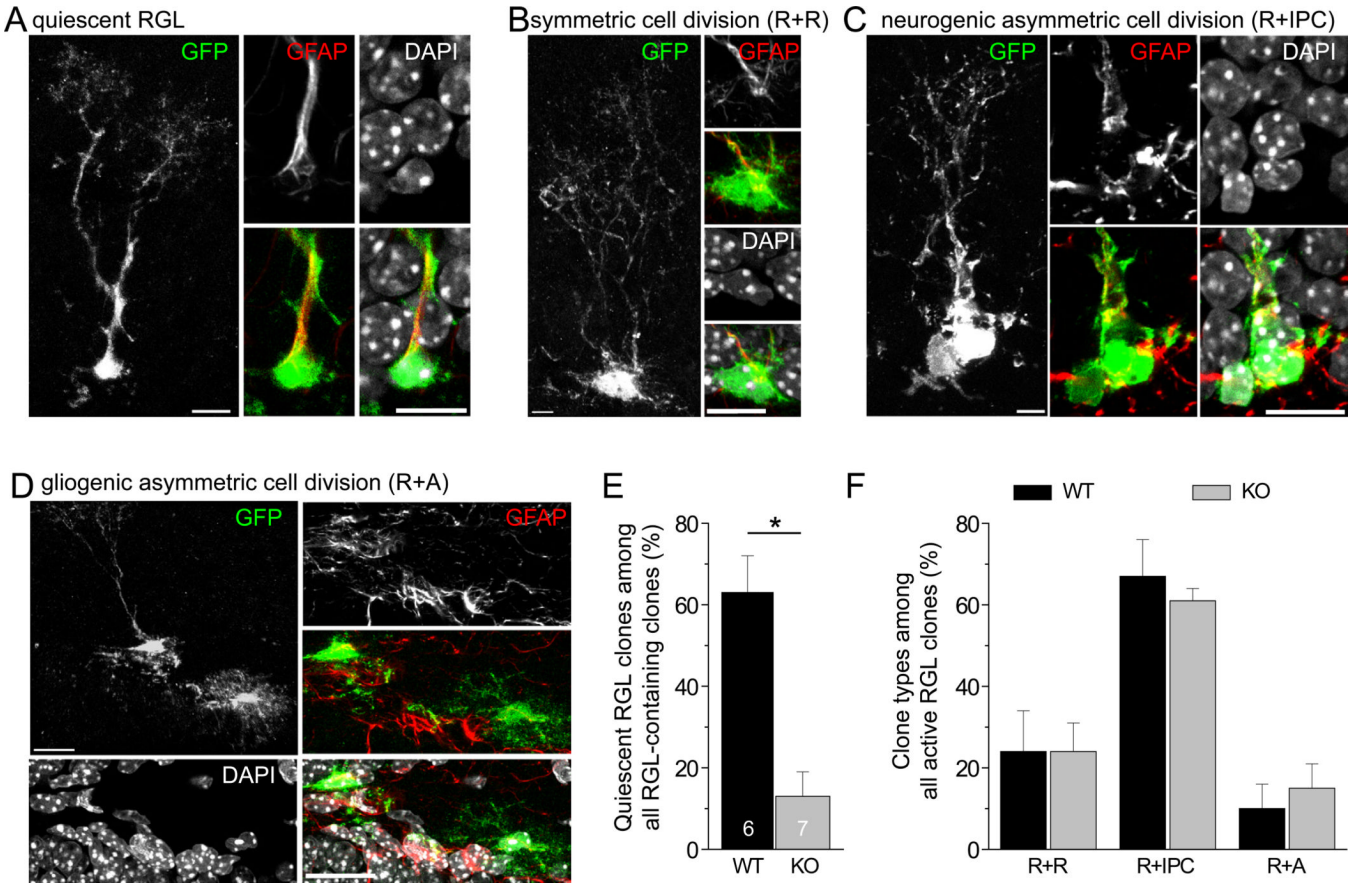

Figure 2. Increased Activation of Quiescent Radial Glia-like Neural Stem Cells in the Dentate Gyrus of Adult *sfrp3* Knockout Mice

(A-D) Sample confocal images of different types of GFP$^+$ clones at 7 dpi. Adult *nestin-CreER$^{T2+/-}$::Z/EG$^{f/+}$::sfrp3$^{-/-}$* KO mice and *nestin-CreER$^{T2+/-}$::Z/EG$^{f/+}$::sfrp3$^{+/+}$* control mice were injected with a single low dose of tamoxifen (62 mg/kg body weight, i.p.) and examined 7 days later. Shown are sample confocal images of immunostaining of GFP and GFAP for a quiescent clone with a single radial glia-like neural stem cell (RGL; A) and for activated clones with two RGLs (B), one RGL and one GFAP$^-$ intemediate procursor cell (IPC; C), and one RGL and one GFAP$^+$ astrocyte with bushy morphology (A; D). Scale bars: 10 μm.

(E) Decreases RGL quiescence in the dentate gyrus of adult *sfrp3* KO mice examined at 7 dpi. Values represent mean ± SEM (n = 6 WT and 7 KO mice; *: $P < 0.01$; student's t-test)

(F) No difference in percenatges of different types of activated clones in adult *sfrp3* KO mice examined at 7 dpi. Values represent mean ± SEM. Same sets of animals as in (E) were used.

See also Figure S2 and Table S1.

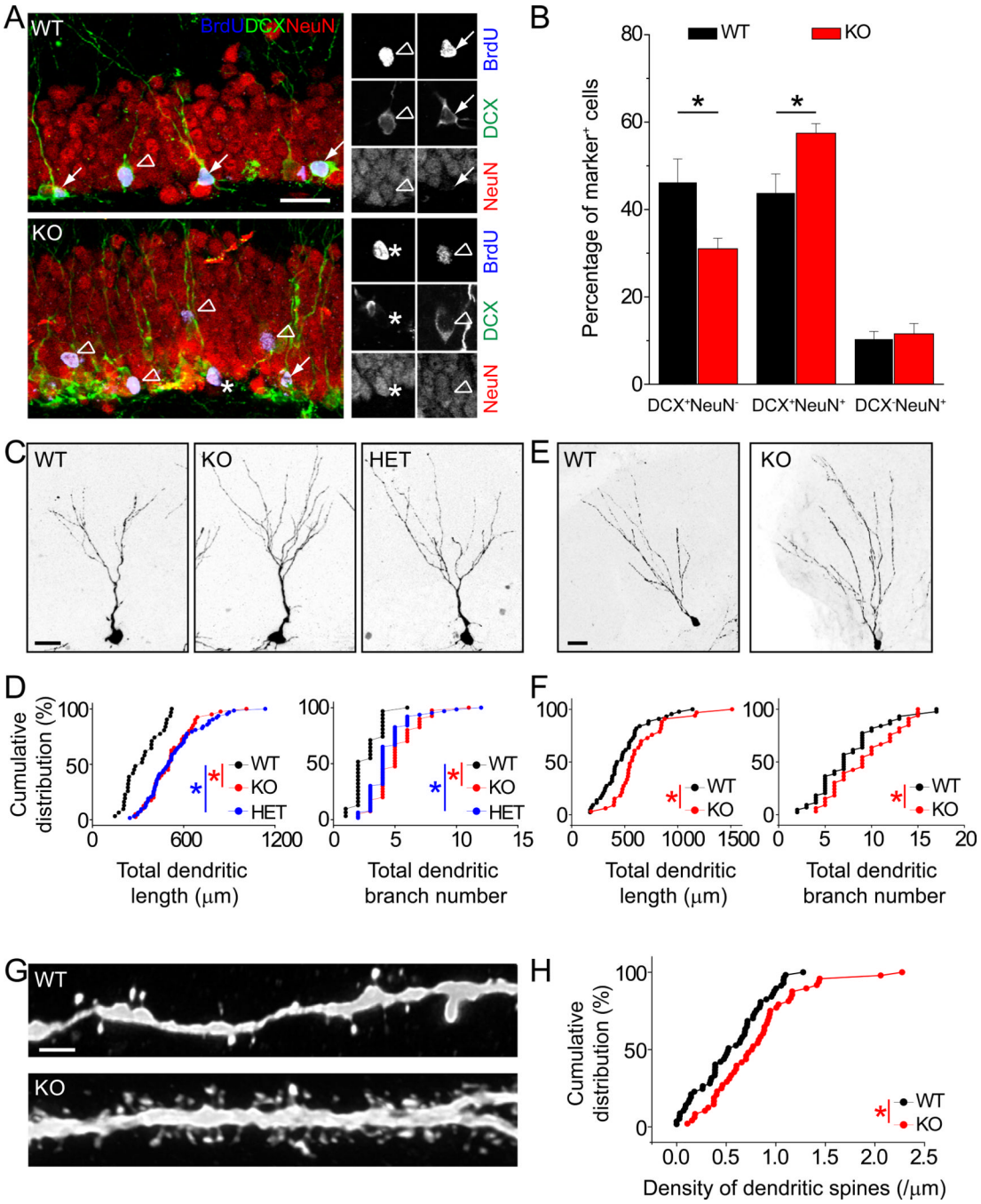

Figure 3. Regulation of Maturation, Dendritic Development and Spine Formation of Newborn Neurons in the Adult Hippocampus by sFRP3

(A-B) Accelerated new neuron maturation in the dentate gyrus of adult *sfrp3* KO mice. Adult mice were injected with BrdU once daily for 1 week and analyzed 2 weeks after the first BrdU injection. Shown in (A) are sample confocal images of BrdU, DCX and NeuN immunostaining. Arrows point to $BrdU^{+}DCX^{+}NeuN^{-}$ immature newborn neurons; arrowheads point to $BrdU^{+}DCX^{+}NeuN^{+}$ more developed newborn neurons; and asterisks point to $BrdU^{+}DCX^{+}NeuN^{-}$mature new neurons. Scale bar: 20 μm. Shown in (B) is a summary of the distribution of newborn neurons at different maturation stages. Values represent mean ± SEM (n = 9 animals each group; *: $P < 0.01$; one-way ANOVA).

(C-G) Accelerated dendritic growth and spine formation of newborn neurons in the dentate gyrus of adult *sfrp3* KO mice. Retroviruses expressing GFP were stereotaxically injected into the dentate gyrus of adult *sfrp3* KO, HET and WT littermates. GFP^+ neurons were examined at 14 dpi (C-D) or 21 dpi (E-H). Shown are sample projected confocal images of GFP^+ newborn neurons at 14 dpi (C) and 21 dpi (E) and dendritic spines at 21 dpi (G). Scale bars: 20 mm. Also shown are cumulative distribution plots of total dendritic length, branch number and spine density of newborn neurons under different conditions (D, F and H). Each symbol represents data from a single GFP^+ neuron (*: $P < 0.01$, Kolmogorov-Smirnov test; n = 3 animals each).
See also Figure S3 and Table S1.

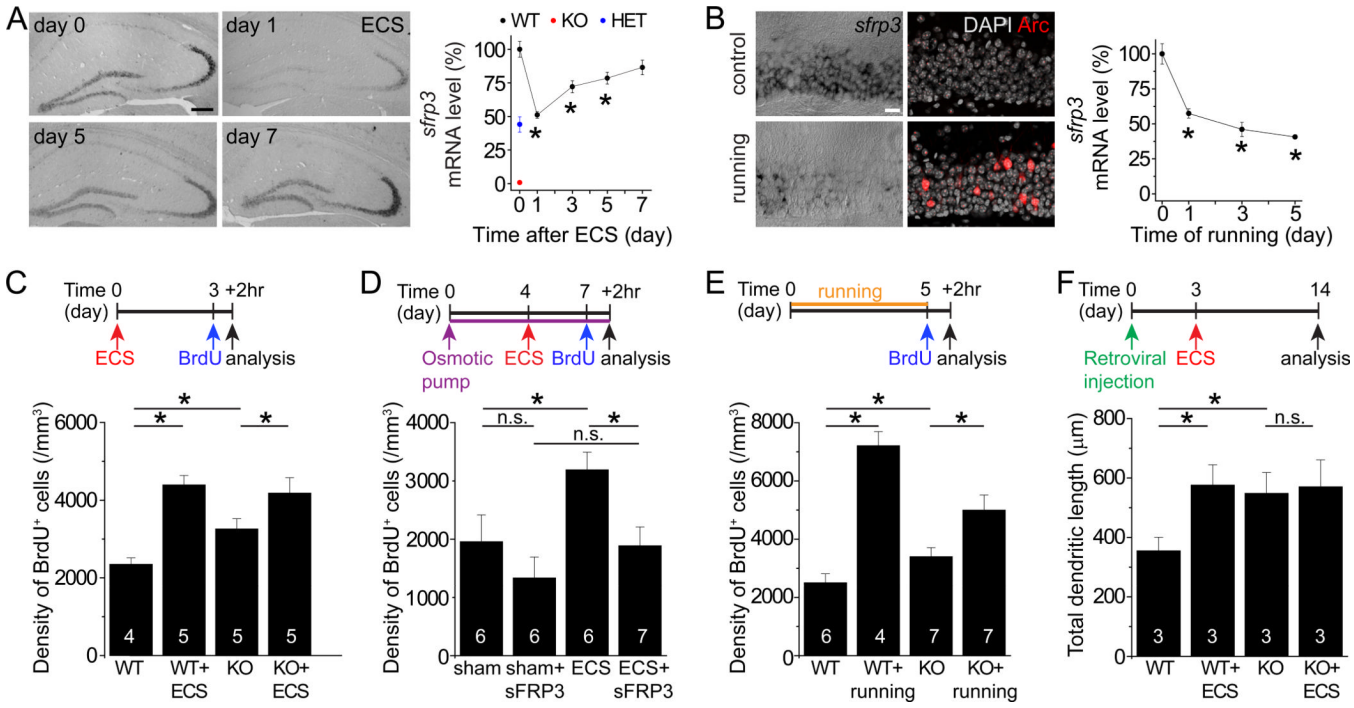

Figure 4. *sfrp3* Reduction of *sfrp3* Mediates Activity-dependent Adult Neurogenesis

(A) ECS decreases *sfrp3* expression in the adult dentate gyrus. Shown are sample images of *sfrp3* in situ in the adult hippocampus at different time after a single ECS (left; scale bar: 200 μm) and quantification by quantitative real-time PCR. Values are normalized to that of sham-treated WT animals at each time point and represent mean ± SEM (n > 3 animals for each time point; *: $P < 0.01$; student's t-test).

(B) Running activates dentate granule neurons and decreases *sfrp3* expression. Shown are sample images of dual *sfrp3* in situ and Arc immunostaining (left; scale bar: 20 μm) and quantification by quantitative real-time PCR (right). Values are normalized to that of sham-treated WT animals and represent mean ± SEM (n ≥ 3 animals for each time point; *: $P < 0.01$; student's t-test).

(C) *sfrp3* deletion-induced increase of progenitor proliferation significantly occludes the ECS effect in the adult SGZ. Shown are schematic diagram of experimental design and stereological quantification of $BrdU^+$ cells in the adult SGZ after a single ECS. Values represent mean ± SEM (*: $P < 0.05$; one-way ANOVA).

(D) Exogenous sFRP3 blocks ECS-induced neural progenitor proliferation in adult WT mice. Shown are schematic diagram of experimental design and stereological quantification of $BrdU^+$ cells in the adult SGZ under different conditions. Values represent mean ± SEM (*: $P < 0.05$; n.s.: $P > 0.1$; one-way ANOVA).

(E) Running-induced increase of cell proliferation is attenuated in the adult *sfrp3* KO mice. Same as in (C), except that mice were subjected to voluntary running.

(F) *sfrp3* deletion-induced dendritic growth of newborn neurons completely occludes the ECS effect. Same as in (C), except that dendritic growth of retrovirally labelled new neurons were analyzed at 14 dpi.

See also Figure S4 and Table S1.